Regional Folding, Quartz Veining and Gold Mineralization in a Metasedimentary Basin along the Malartic Segment of the Larder Lake–Cadillac Deformation Zone, Abitibi Greenstone Belt, Quebec

B. Samson, B. Lafrance and X. Zhou

Mineral Exploration Research Centre, Harquail School of Earth Sciences, Laurentian University, Sudbury, Ontario, P3E 2C6

INTRODUCTION

The Larder Lake–Cadillac deformation zone (LLCDZ; Figure 1) in the Abitibi greenstone belt of the Archean Superior Province is a major crustal-scale deformation zone hosting numerous world-class gold deposits. Little work has been done on gold mineralization within the metasedimentary basin along the Malartic segment of the LLCDZ due to the lack of outcrop. However, new outcrops stripped mechanically by Midland Exploration Inc. and IAMGOLD Corp. over the last three years, as well as logging in the fall of 2017, provide a new opportunity to study gold mineralization in this prospective district. An area along the Malartic segment of the LLCDZ (Figure 2) was mapped in the summer of 2018 as part of the Malartic seismic-transect mapping project of the Metal Earth research initiative.

The goals of this 2018 mapping project were to confirm the structural history of the basin, determine the relative timing of the quartz veining and establish the significance of a newly found quartz-feldspar porphyry along the LLCDZ. This report summarizes preliminary results from the field mapping, with emphasis on the structural history of the supracrustal rocks, the gold-bearing veins and their relative timing with respect to regional folding.

REGIONAL SETTING

The Abitibi greenstone belt comprises volcanic and sedimentary assemblages intruded by large granitoid bodies. Four volcanic units occur in close proximity to the LLCDZ: the Piché (2709–2706 Ma; Pilote et al., 2015), Malartic (2714–2704 Ma; Pilote et al., 1999, 2015), Louvicourt (2704 Ma; Pilote et al., 1999, 2015) and Blake River (2703–2695 Ma; Corfu et al., 1989, 1993; Mortensen, 1993; McNicoll et al., 2014) groups (Bedeaux et al., 2017). The Piché group occurs along the LLCDZ and consists mainly of strongly deformed ultramafic and mafic volcanic rocks (Latulippe, 1976; Simard et al., 2013), with minor intermediate andesitic rocks (Landry, 1991). The Malartic group consists of ultramafic and mafic volcanic rocks intercalated with minor intermediate to felsic volcanic rocks, whereas the Louvicourt and Blake River groups consist mostly of mafic and felsic volcanic rocks (Bedeaux et al., 2017).

Two Archean metasedimentary basins along the Malartic segment of the LLCDZ overlie the volcanic units (Thurston et al., 2008; Figure 1). Rocks of the Cadillac group (Dimroth et al., 1982) were deposited in a basin, now exposed over a 150 by 5 km area, unconformably overlying older volcanic rocks of the Blake River group, north of the LLCDZ (Goutier, 1997; Lafrance et al., 2003; Mercier-Langevin et al., 2007, Thurston et al., 2008). The Cadillac group was deposited at ca. 2686 Ma (Mortensen 1993; Davis, 2002) and is equivalent to the Porcupine Assemblage in Ontario (Ayer et al., 2002; Thurston et al., 2008). The Cadillac basin is in turn unconformably overlain by younger fluvial conglomerate, sandstone and shallow marine turbidites of the ca. 2677–2672 Ma Timiskaming Group (Corfu and Davis, 1991; Davis, 2002; Pilote et al., 2015).

The Pontiac Subprovince, which lies immediately south of the LLCDZ and the Abitibi greenstone belt, consists of turbiditic sandstone, minor conglomerate, iron formation, and ultramafic and mafic rocks (Goulet, 1978; Dimroth et al., 1982; Perrouty et al., 2017). Metasedimentary rocks were deposited between ca. 2685 Ma, the age of the youngest detrital zircons in sandstone, and ca. 2682 Ma, the crystallization age of the crosscutting Lac Fournière pluton.

LITHOLOGICAL UNITS AND REGIONAL STRUCTURES

The Cadillac group consists of interlayered turbiditic sandstone and mudstone. Younging indicators include erosional channelling at the base of conglomeratic beds and normal grading in sandstone beds. The younger Timiskaming Group includes alternating horizons of polymictic conglomerate (Figure 3a) and trough-crossbedded sandstone, as well as marine-facies turbiditic sedimentary rocks (Figure 3b). Polymictic conglomeratic beds contain clasts of mafic volcanic rocks, felsic volcanic rocks, granitoids, chert and smoky quartz.

The Cadillac and Timiskaming rocks are overprinted by regional folds with an axial planar regional cleavage striking west-northwest and dipping steeply to the north and south (Figure 4). The regional cleavage is expressed as a continuous slaty cleavage in mudstone, as a spaced disjunctive cleavage in sandstone, and by the flattening and elongation of clasts in conglomerate. It is oriented anticlockwise to north-facing beds (Figure 3b) and clockwise to south-facing beds., Tight to isoclinal, S-shaped and Z-shaped parasitic folds (Figure 3c) are present on opposite limbs of the regional folds. The parasitic folds plunge moderately to shallowly to the east-southeast parallel to a mineral stretching lineation, which is defined by biotite porphyroblasts in turbiditic sandstone (Figures 3d) and elongation of clasts in conglomerate. Two stripped mineralized outcrops, TR16-10 (Figure 5) and TR16-02 (Figure 6), which are located on opposite limbs of a regional fold, were mapped in detail and are described below.

Stripping TR16-10 (708141E, 5341183N; UTM Zone 17, NAD83)

Stripping TR16-10 is located on the north-younging northern limb of a regional anticline. It consists of turbiditic siltstone and mudstone and thick-bedded sandstone. Beds strike ~290˚ and dip steeply to the north. The steeply-dipping regional cleavage strikes 280˚ anticlockwise to bedding. A mineral stretching lineation is parallel to parasitic fold axes and plunges moderately toward the east-southeast (105˚).

Four generations of quartz veins (V1 to V4) are present on outcrop. The V1 veins (Figure 7a) only occur in the thicker sandstone beds, where they form en-échelon arrays oriented roughly parallel to the cleavage. They consist of smoky quartz and vary in width from ~2 mm to 3 cm. The V2 veins (Figure 7b) are tension gashes composed of quartz, albite, Fe-carbonate and biotite, and vary in width from 2 to 5 cm, with an average length of ~10 cm. They strike 190˚ and dip moderately to the west, subperpendicular to the mineral stretching lineation. The V3 veins (Figure 7c) are sigmoidal en-échelon veins, which are also restricted to the more competent thicker sandstone beds, consist of smoky to white quartz and vary in width from 2 to 10 cm. The V4 veins (Figure 7d, e) are extensional veins composed of black smoky quartz and white quartz. Reaching up to several metres in length and 25 cm in width, these veins extend for hundreds of metres. They strike 100˚, are oriented at a low angle anticlockwise to bedding and are overprinted by tight S-shaped folds. They are surrounded by an alteration halo of chlorite, arsenopyrite, carbonate, tourmaline and biotite, which extends over 5 to 10 cm on both sides of the veins. The V4 veins and their alteration haloes are gold-bearing and returned gold assay values of 1.7–41 g/t Au (Midland Exploration Inc., 2016).

The orientation of the V3 and V4 veins anticlockwise to bedding, the sigmoidal shape of the V3 veins and the overprinting of the V4 veins by S-shaped folds are consistent with the emplacement of the veins during sinistral shearing. The veins were deformed during a subsequent deformation event. The V4 veins are boudinaged, offset by steeply-dipping dextral shear bands and overprinted by Z-shaped drag folds, due to later dextral shearing parallel to bedding (Figure 7e).

Stripping TR16-02 (706373E, 5341667N; UTM Zone 17, NAD 83)

Stripping TR16-02 is located on the south-younging southern limb of the regional anticline, where the regional cleavage is defined by flattened clasts oriented clockwise to bedding. The stripping consists of polymictic Timiskaming conglomerate interlayered with massive and normal-graded sandstone. The beds strike 280˚ and dip steeply to the north. The subvertical cleavage strikes ~290˚ and is oriented clockwise to bedding. A mineral stretching lineation defined by elongated clasts plunges moderately to shallowly toward ~100˚.

Only V2 and V4 veins are present on this outcrop. The V2 veins are oriented (~160˚/60˚) roughly perpendicular to the mineral stretching lineation (Figure 8a), whereas the S-folded V4 veins are east–west oriented anticlockwise to bedding (Figure 8b). The V4 veins are boudinaged and overprinted by dextral shear bands (Figure 8c). Granitic clasts in conglomerate are surrounded by dextral asymmetrical strain shadows and locally filled with hydrothermal minerals (Figure 8d).

SUMMARY AND CONCLUSION

The regional isoclinal folds and their axial plane cleavage formed during a north-northeast–directed shortening event. The V1 veins were emplaced prior to folding and were rotated into the orientation of the axial plane cleavage. The V2 veins were emplaced during folding as tension gashes oriented subperpendicularly to the stretching lineation. During subsequent progressive sinistral shear, the V3 veins formed as arrays of tension gashes that were curved into S-shaped folds during continued shear. The gold-bearing V4 quartz veins filled fractures oriented anticlockwise to bedding and were then folded to form an S-like shape. As the V4 veins are oriented anticlockwise to bedding on both limbs of the fold, this suggests that they formed after regional folding. Later dextral shearing parallel to bedding produced dextral shear bands, boudinage structures and dextral drag folds overprinting the V4 veins.

At the nearby Canadian Malartic gold deposit located south of the LLCDZ, gold mineralization is controlled by structures that formed during regional sinistral folding of the Pontiac metasedimentary rocks (De Souza et al., 2016). As gold mineralization in the Cadillac and Timiskaming basins is also associated with sinistral structures, its emplacement could be structurally coeval or slightly later than that of gold mineralization at the Canadian Malartic deposit.

ACKNOWLEDGMENTS

Both G Roger, President and CEO of Midland Exploration Inc., and M.-F. Bugnon, General Manager Exploration of IAMGOLD Corp., are thanked for allowing access to the Héva East property. The authors are grateful for the discussion on interpretations throughout the summer with P. Pilote of the Ministère de l'Énergie et des Ressources naturelles du Québec, as well as R. Daigneault from the Université du Québec à Chicoutimi and S. De Souza from the Université du Québec à Montréal. Lastly but not least, L. Roy is thanked for his hard work and assistance throughout the field season.

Harquail School of Earth Sciences, Mineral Exploration Research Centre contribution MERC-ME2018-066

REFERENCES

Ayer, J., Amelin, Y., Corfu, F., Kamo, S., Ketchum, J., Kwok, K. and Trowell, N. 2002. Evolution of the southern Abitibi greenstone belt base on U-Pb geochronology: autochthonous volcanic construction followed by plutonism, regional deformation and sedimentation; Precambrian Research, v. 115, p. 63–95.

Bedeaux, P., Pilote, P., Daigneault, R. and Rafini, S. 2017. Synthesis of the structural evolution and associated gold mineralization of the Cadillac Fault, Abitibi, Canada; Ore Geology Reviews; v. 82, p. 49–69.

Corfu, F. and Davis, D.W. 1991. Comment on "Archean hydrothermal zircon in the Abitibi greenstone belt: constraints on the timing of gold mineralization" by J.C. Claoué-Long, R.W. King and R. Kerrich; Earth and Planetary Science Letters, v. 104, p. 545–552.

Corfu, F., Krogh, T.E., Kwok, Y.Y. and Jensen, L.S. 1989. U–Pb zircon geochronology in the southwestern Abitibi greenstone belt, Superior Province; Canadian Journal of Earth Sciences, v. 26, p. 1747–1763.

Corfu, F., Spooner, E.T.C. and Barrie, C.T. 1993. The evolution of the southern Abitibi greenstone belt in light of precise U-Pb geochronology; Economic Geology, Bulletin of the Society of Economic Geologists, v. 88, p. 1323–1340.

Davis, D.W. 2002. U-Pb geochronology of Archean metasedimentary rocks in the Pontiac and Abitibi subprovinces, Quebec, constraints on timing, provenance and regional tectonics; Precambrian Research, v. 115, p. 97–117.

De Souza, S., Dubé, B., McNicoll, V., Dupuis, C., Mercier-Langevin, P., Creaser, R. and Kjarsgaard, I. 2016. Geology and hydrothermal alteration of the world-class Canadian Malartic gold deposit: genesis of an Archean stockwork-disseminated gold deposit in the Abitibi greenstone belt, Quebec; chapter 9 *in* Archean Base and Precious Metal Deposits, Southern Abitibi Greenstone Belt, Canada, T. Monecke, P. Mercier-Langevin, B. Dubé (ed.); Reviews in Economic Geology, v. 19, p. 263–276.

Desrochers, J.P. and Hubert, C. 1996. Structural evolution and early accretion of the Archean Malartic Composite Block, southern Abitibi greenstone belt, Quebec, Canada Canadian Journal of Earth Sciences, v. 33, p. 1556–1569.

Desrochers, J.P., Hubert, C., Ludden, J.N. and Pilote, P. 1993. Accretion of Archean oceanic plateau fragments in the Abitibi greenstone belt, Canada; Geology, v. 21, p. 451–454.

Dimroth, E., Imreh, L., Rocheleau, M. and Goulet, N. 1982. Evolution of the south-central part of the Archean Abitibi Belt, Quebec. Part I: stratigraphy and paleogeographic model; Canadian Journal of Earth Sciences, v. 19, p. 1729–1758.

Goulet, N. 1978. Stratigraphy and structural relationships across the Cadillac-Larder Lake Fault, Rouyn-Beauchastel area, Quebec; Ph.D. thesis, Queen's University, Kingston, Ontario, 286 p.

Goutier, J. 1997. Géologie de la région de Destor; Ministère des Ressources naturelles du Québec, report RG 96-13, 37 p.

Hubert, C., Trudel, P. and Gelinas, L. 1984. Archean wrench fault tectonics and structural evolution of the Blake River group, Abitibi belt, Quebec; Canadian Journal of Earth Sciences, v. 21, 1024–1032.

Hyde, R.S. 1980. Sedimentary facies in the Archean Timiskaming Group and their tectonic implications, Abitibi greenstone belt, northeastern Ontario, Canada; Precambrian Research, v. 12, p. 161–195.

Imreh, L. 1984. Sillon de La Motte–Vassan et son avant-pays méridional: synthèse volcanologique, lithostratigraphique et gîtologique; Ministère de l'Énergie et des Ressources du Québec, Direction générale de l'exploration géologique et minérale, MM82-4, 72 p., 2 maps.

Lafrance, B., Moorhead, J. and Davis, D.W. 2003. Cadre géologique du camp minier de Doyon-Bousquet-Laronde: Ministère des Ressources naturelles, de la Faune et des Parcs du Québec, report ET 2002-07, 43 p.

Landry, J. 1991. Volcanologie physique et sédimentologie du groupe volcanique de Piché et relations stratigraphiques avec les groupes sédimentaires encaissants de Pontiac et de Cadillac; unpublished M.Sc. thesis, Université du Québec à Chicoutimi, Chicoutimi, Quebec, 210 p.

Latulippe, M. 1976. Excursion géologique: la région de Val d'Or–Malartic; Ministère des Richesses naturelles du Québec (ed.), Institut canadien des mines et de la métallurgie, DPV-367, 129 p.

McNicoll, V., Goutier, J., Dubé, B., Mercier-Langevin, P., Ross, P.-S., Dion, C., Monecke, T., Legault, M., Percival, J. and Gibson, H. 2014. U–Pb Geochronology of the Blake River Group, Abitibi greenstone belt, Quebec, and implications for base metal exploration; Economic Geology, v. 109, p. 27–59.

Mercier-Langevin, P., Dubé, B., Hannington, M.D., Richer-Laflèche, M. and Gosselin, G. 2007. The LaRonde Penna Au-rich volcanogenic massive sulfide deposit, Abitibi greenstone belt, Quebec: Part II. Lithogeochemistry and paleotectonic setting; Economic Geology, v. 102, p. 611–631.

Midland Exploration Inc. 2016. Midland continues to discover several new gold-bearing zones on its Heva project, with grades up to 41.0 g/t Au by prospecting; news release, December 20, 2016, http://www.midlandexploration.com/en/Communique.aspx?ResourceId=31fa1039-8a5a-4807-a8c7-2ea5bc814052 [last accessed: September 2018].

Mortensen, J.K. 1993. U-Pb geochronology of the eastern Abitibi Subprovince. Part 2: Noranda–Kirkland Lake area; Canadian Journal of Earth Sciences, v. 30, p. 29–41.

Perrouty, S., Gaillard, N., Piette-Lauzière, N., Mir, R., Bardoux, M., Olivo, G.R., Linnen, R., Bérubé, C., Lypaczewski, P., Guilmette, C., Feltrin, L. and Morris, W. 2017. Structural setting for Canadian Malartic style of gold mineralization in the Pontiac Subprovince, south of the Cadillac Larder Lake Deformation Zone, Québec, Canada; Ore Geology Reviews, v. 84, p. 185–201.

Pilote, P. 2013. Géologie Malartic, 32D01-NE; Ministère de l'Énergie et des Ressources naturelles du Québec, CG-32D01D-2013-01.

Pilote, P., Daigneault, R., David, J. and McNicoll, V. 2015. Architecture of the Malartic, Piché and Cadillac groups and the Cadillac Fault: geological revisions, new dates and interpretations; Ministère de l'Énergie et des Ressources naturelles du Québec, DV 2015-04. 37 p.

Pilote, P., Scott, C.R., Mueller, W., Lavoie, S. and Riopel, P. 1999. Géologie des formations de Val-d'Or, Héva et Jacola: nouvelle interprétation du groupe de Malartic; *in* Explorer au Québec : le défi de la connaissance. Séminaire d'information sur la recherche géologique, programme et résumés, 1999; Ministère de l'Énergie et des Ressources, DV 99-03, 52 p.

Simard, M., Gaboury, D., Daigneault, R. and Mercier-Langevin, P. 2013. Multistage gold mineralization at the Lapa mine, Abitibi Subprovince: insights into auriferous hydrothermal and metasomatic processes in the Cadillac–Larder Lake Fault Zone; Mineral Deposits, v. 48, p. 883–905.

Thurston, P.C., Ayer, J.A., Goutier, J. and Hamilton, M.A. 2008. Depositional gaps in Abitibi greenstone belt stratigraphy: a key to exploration for syngenetic mineralization; Economic Geology, v. 103, p. 1097–1134.

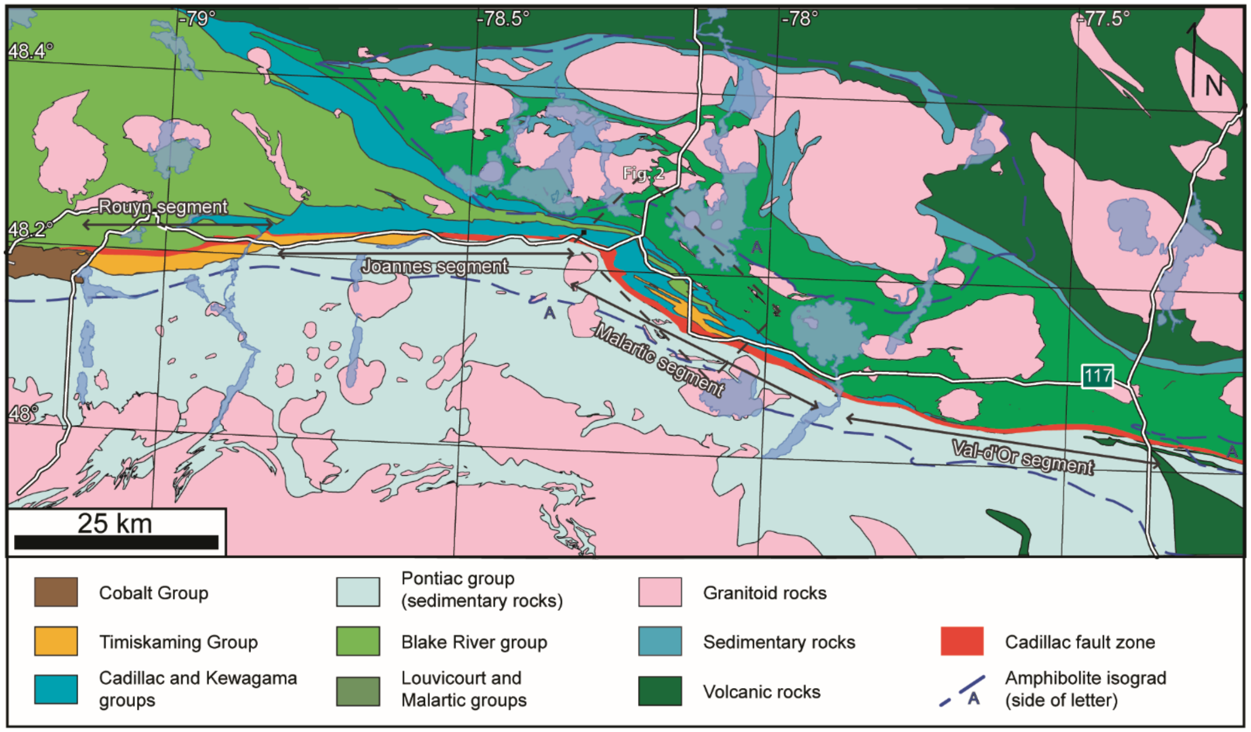

Figure 1. Regional geology of the Larder Lake–Cadillac deformation zone (LLCDZ) subdivided into four segments. Figure *modified from* Hubert et al. (1984), Imreh (1984), Desrochers and Hubert (1996) and Bedeaux et al. (2017).

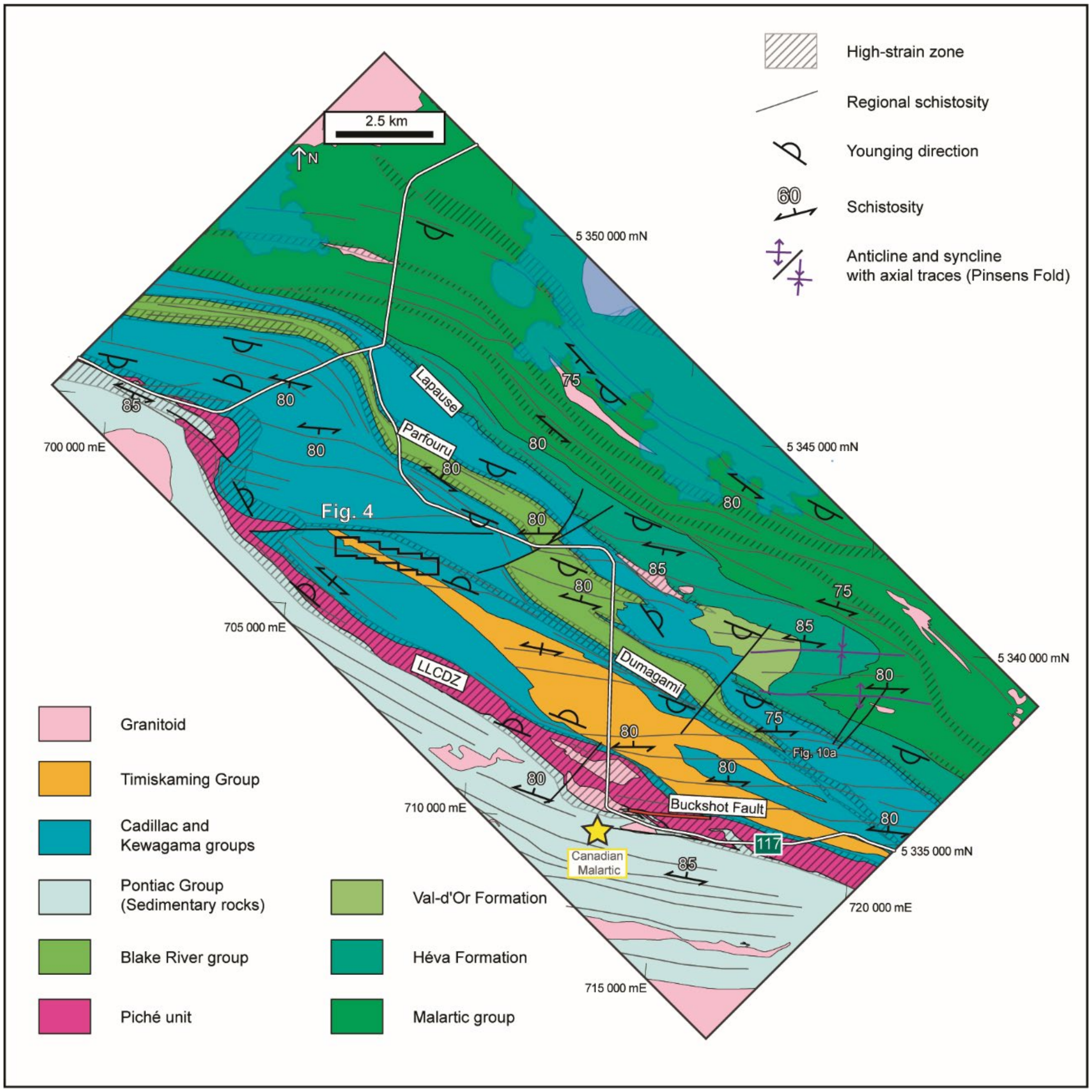

Figure 2. Geology of the Malartic segment of the Larder Lake–Cadillac deformation zone (LLCDZ). Figure *modified from* Desrochers et al. (1993), Desrochers and Hubert (1996), Pilote et al. (1999), Pilote (2013), Pilote et al. (2015) and Bedeaux et al. (2017). Outline in black shows location of Figure 4.

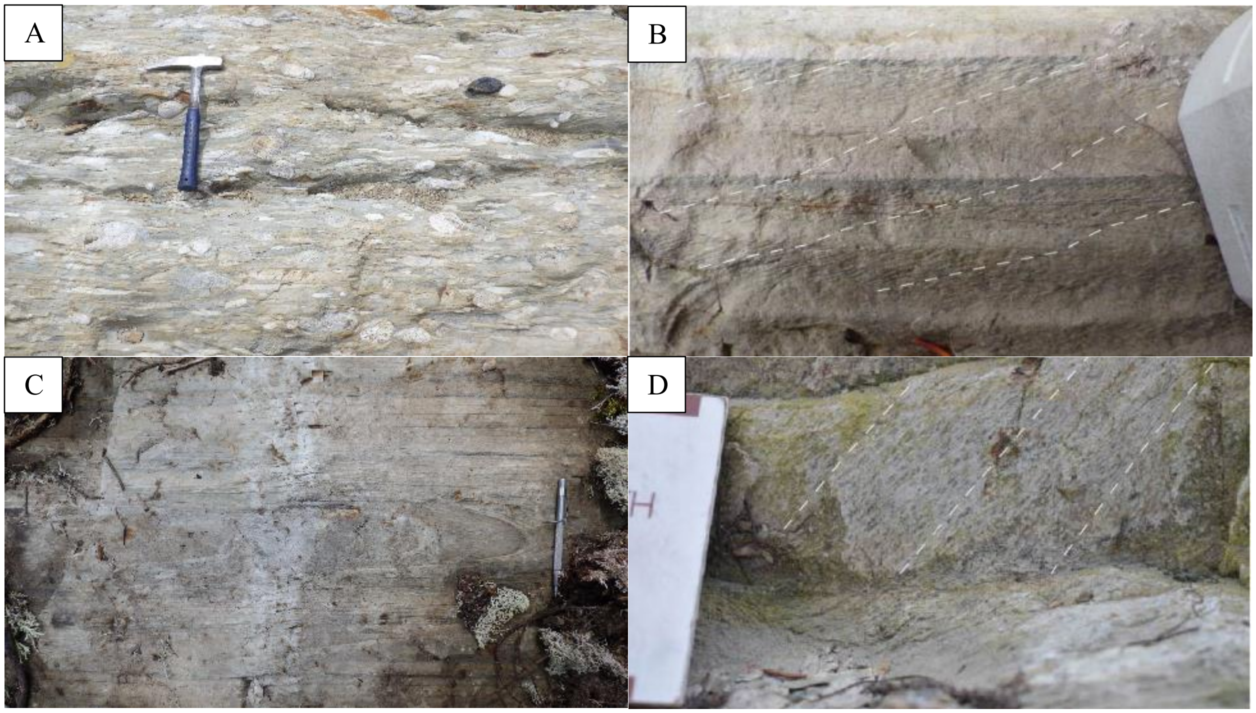

Figure 3. Field photographs of the lithological units of the Timiskaming Group in the Abitibi greenstone belt: **a)** typical Timiskaming polymictic conglomerate (hammer is 33 cm long); **b)** north-younging, normal-graded turbiditic sandstone of the Timiskaming Group overprinted by an anticlockwise cleavage indicated by white dashed lines (compass is 7 cm long); **c)** isoclinal fold parasitic to regional folds (pen magnet is 13 cm long); **d)** biotite porphyroblasts define regional stretching lineation indicated by white dashed lines (photo card is 5 cm in width).

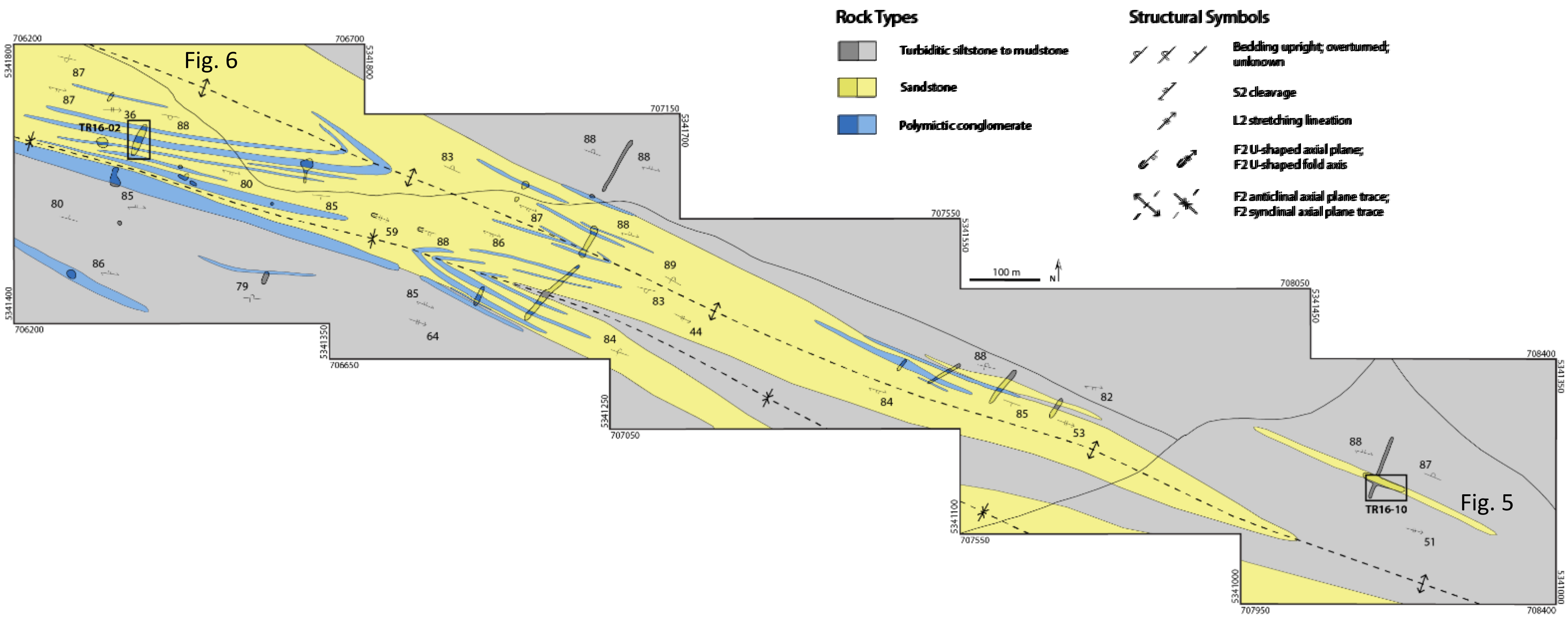

Figure 4. Geological map, showing regional isoclinal anticline and syncline in Timiskaming conglomerate, sandstone and turbidites at 1:2000 scale.

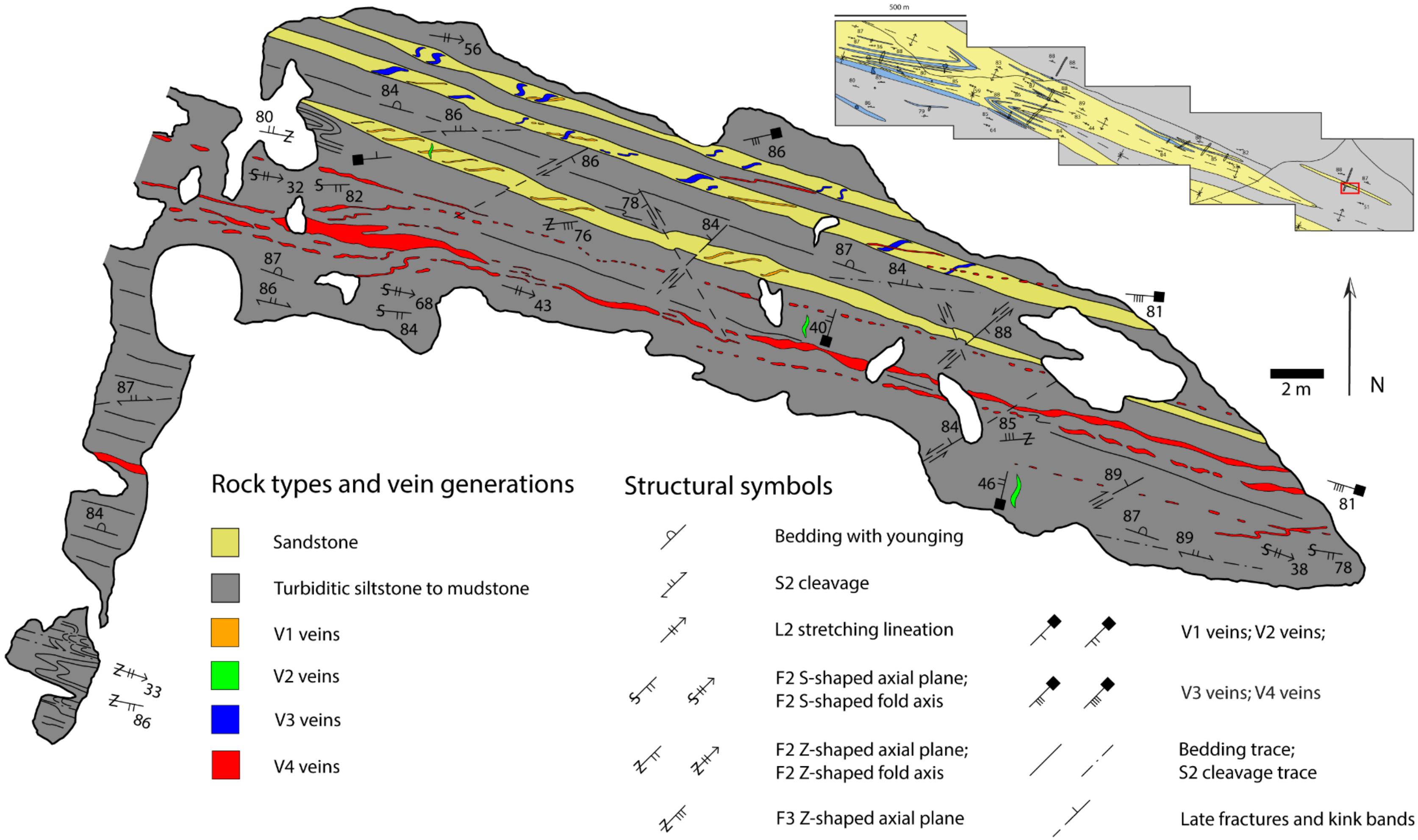

Figure 5. Geology of stripped mineralized outcrop TR16-10 located on the northern limb of a regional anticline of the Abitibi greenstone belt. Bedding is younging toward the north on this outcrop, with the cleavage oriented anticlockwise to the bedding. The gold-bearing V4 quartz veins are shown in red. Inset shows location of outcrop on Figure 4.

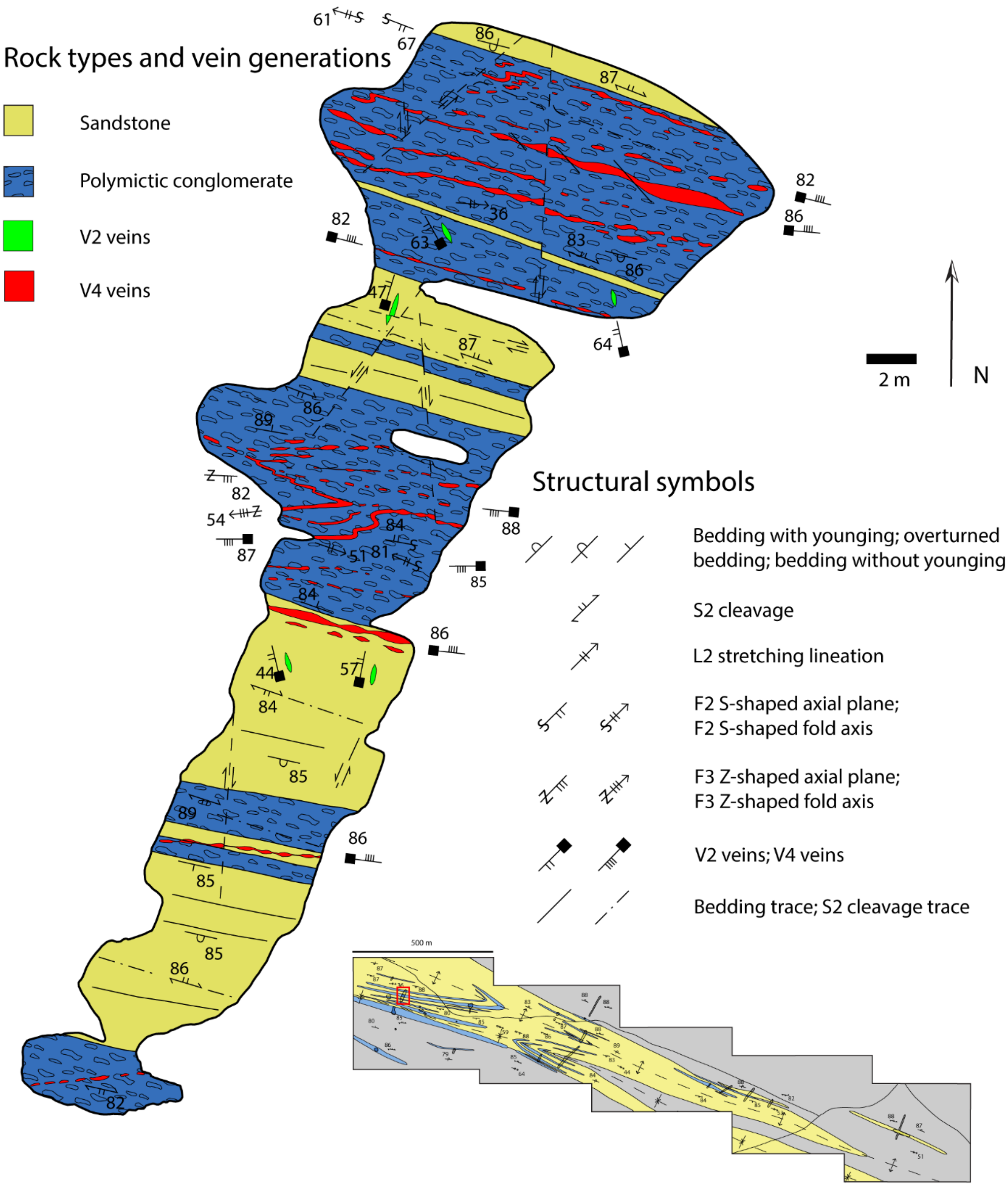

Figure 6. Geology of stripped mineralized outcrop TR16-02 located on the southern limb of a regional anticline of the Abitibi greenstone belt. Bedding is younging toward the south, with the cleavage oriented clockwise to the bedding. Gold-bearing V4 veins are shown in red. Inset shows location of outcrop on Figure 4.

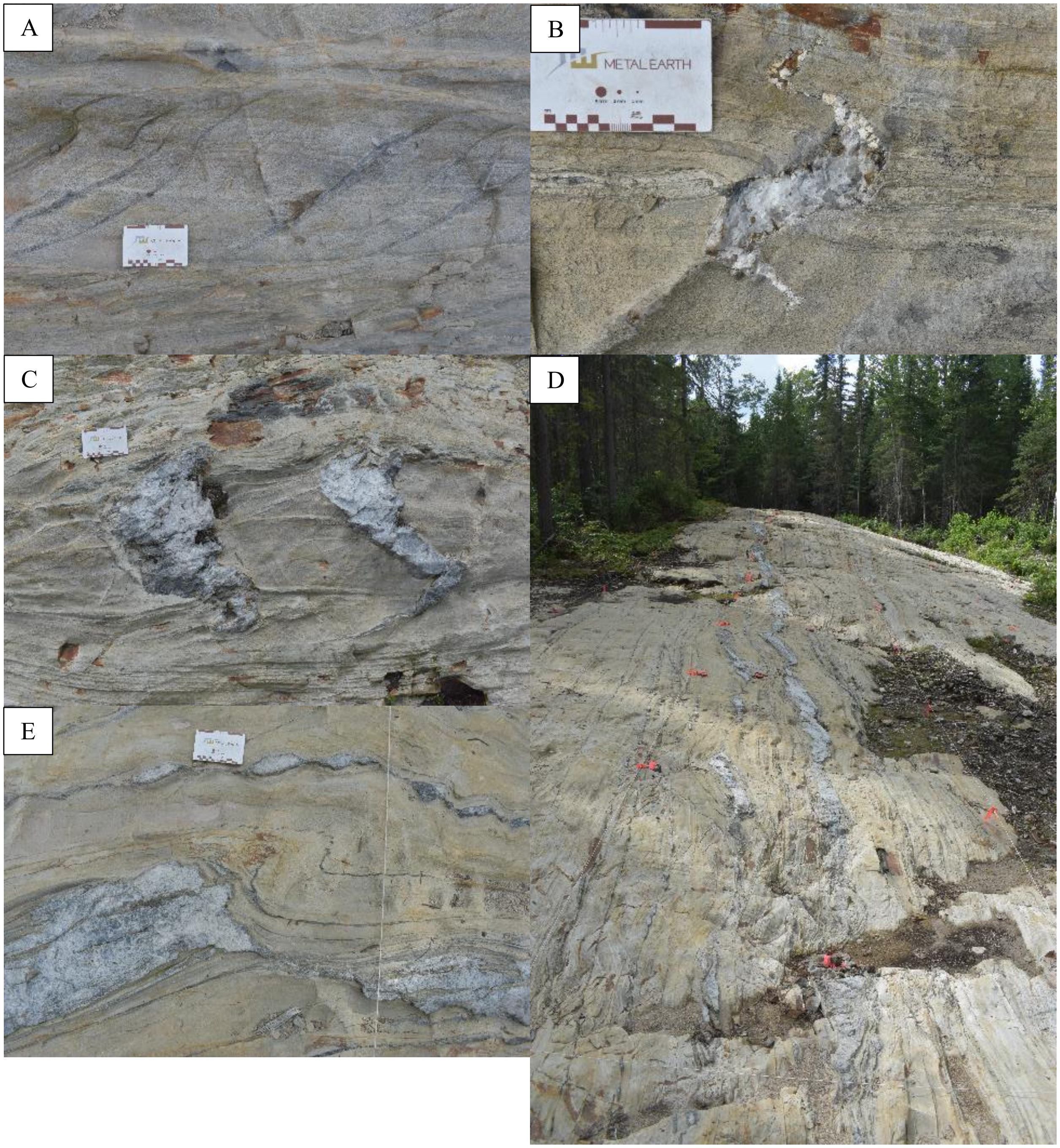

Figure 7. Field photographs of V1 to V4 veins on stripped mineralized outcrop TR16-10 located on the northern limb of a regional anticline of the Abitibi greenstone belt: **a)** dark quartz, en-échelon V1 veins (photograph card measures 8 cm); **b)** Z-shaped V2 tension gash (photograph card measures 8 cm); **c)** smoky to white quartz, S-shaped V3 veins (photograph card measures 8 cm); **d)** smoky to white quartz, extensional V4 veins oriented at a low angle anticlockwise to bedding (spacing between orange flagging is 2 m); **e)** boudinaged V4 veins overprinted by dextral shear bands and flanked by late Z-folds (photograph card measures 8 cm).

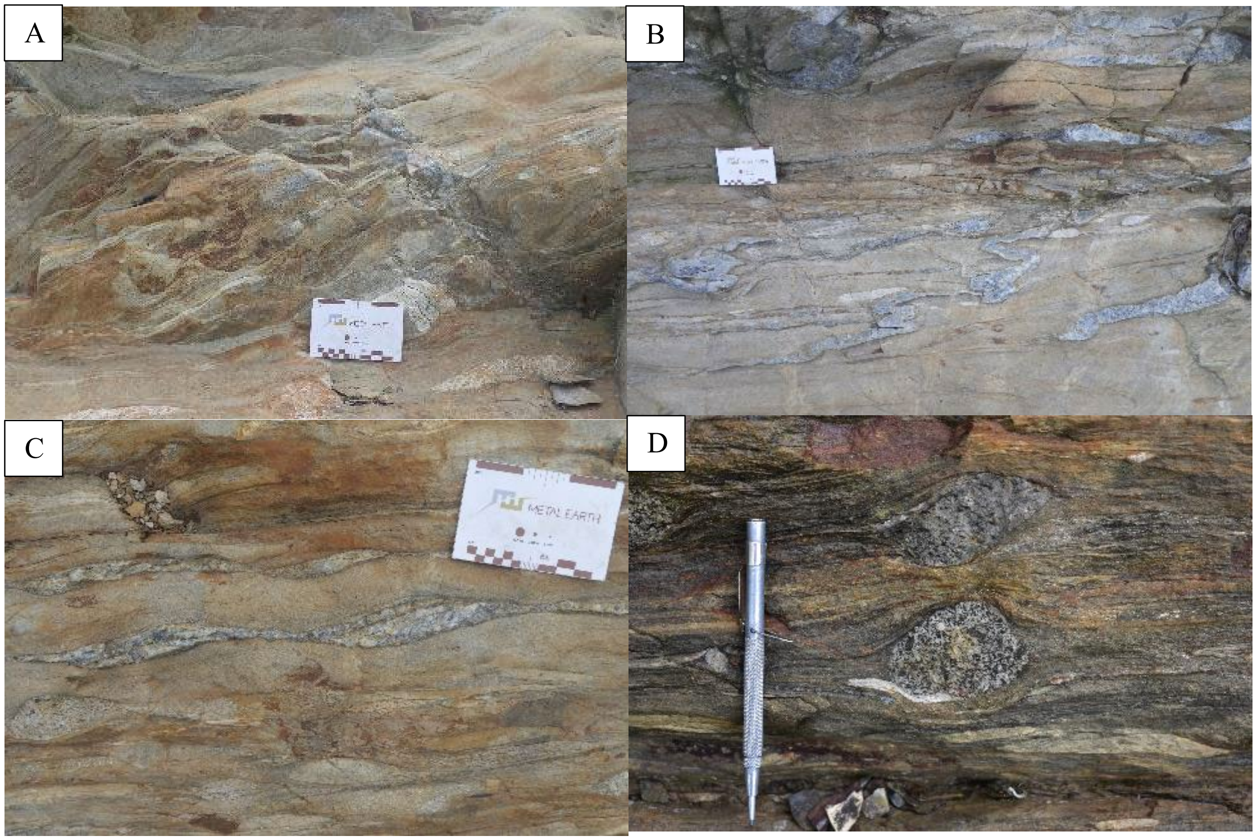

Figure 8. Field photographs from stripped mineralized outcrop TR16-02 located on the southern limb of a regional anticline of the Abitibi greenstone belt: **a)** V2 vein oriented subperpendicularly to the stretching lineation (photograph card measures 8 cm); **b)** S-folded V4 vein oriented anticlockwise to bedding (photograph card measures 8 cm); **c)** V4 veins, which have been boudinaged and cut by dextral shear bands (photograph card measures 8 cm); **d)** Dextral asymmetrical strain shadows surrounding granitoid clasts in conglomerate (pen magnet is 13 cm long).